1. SUPPLEMENTARY FIGURE LEGENDS

Supplementary Figure 1 (S1; related to Figure 1): GIV and Gαi3 localize at the Golgi. (A, B) GIV and Gαi3 colocalize with β-COP, and with each other in the perinuclear Golgi region. **(A)** COS7 cells were stained for endogenous GIV (red, upper panel) or Gαi3 (red, lower panel) and β-COP (green) and analyzed by confocal microscopy. Yellow pixels in merge panels show that β-COP is concentrated in the Golgi where it overlaps with GIV and Gαi3. GIV and Gαi3 are found at the PM (arrowheads) as well as the Golgi, where they were previously shown to localize (Ghosh et al., 2010; Ghosh et al., 2008). Bar = 10 μm. **(B)** COS7 cells were transfected with internally tagged Gαi3-WT-YFP or Gαi3-WF-YFP (pseudocolored in green), fixed and stained for endogenous GIV (red). Yellow pixels in merge panels show that both WT and WF mutant YFP tagged Gαi3 proteins colocalized with GIV in the perinuclear Golgi region. Bar = 10 μm. **(C, D)** Confirmation of effective depletion of GIV using short hairpin (sh) and siRNA oligos. **(C)** Whole cell lysates of COS7 cells stably infected with lentivirus containing scramble (Scr) or GIV shRNA were analyzed for endogenous GIV by immunoblotting (IB). **(D)** Whole cell lysates of COS7 cells acutely transfected with control (Ctrl) or GIV siRNA were analyzed for endogenous GIV by immunoblotting (IB).

Supplementary Figure 2 (S2; related to Figure 2): GIV interacts with subunits of COPI coats. (A) Confirmation of the quality of membrane fractions used for immunoisolation of COPI membranes. Cytosolic (S, 100,000 *g* supernatant) and membrane (P, 100,000 *g* pellet) prepared from postnuclear supernatants (PNS) from COS7 cells were analyzed for GIV, β-COP, Transferrin receptor (TfR) and αTubulin by immunoblotting (IB). These membrane fractions were resuspended and incubated with CM1A10 mAb to immunoisolate COPI membranes in **Fig. 2A**. **(B)** HeLa cells expressing GalT-YFP (Golgi marker, pseudocolored green) were fixed and analyzed for interactions between GIV and β-COP by *in situ* PLA (red) as in **2B**. Representative image of a negative control is displayed, in which the PLA assays were carried out exactly as in **2B**, except the step of incubation with primary antibodies was excluded. **(C)** GIV interacts with β-COP-containing structures in the cell periphery and such interaction is significantly diminished (by 60%) after treatment with BFA. **Left:** HeLa cells were treated with vehicle (left panel) or 5 μg/mL BFA (right panel) for 30 min, and analyzed for interactions between GIV and β-COP by *in situ* PLA. Bar = 10 μm. **Right:** Bar graphs display the quantification of interactions (red dots per cell) shown in **C**. Results are expressed as mean ± S.E.M. of 3 independent experiments (>200

cells/experiment). **(D, E)** GIV interacts with β-COP **(D)**, a subunit of COPI coat, but not with SEC13 **(E)**, a subunit of COPII coat. **(D)** Lysates of COS7 cells transfected with pCEFL-GST-GIV or empty vector (pCEFL-GST) were incubated with glutathione-Sepharose beads and proteins bound to GST/GST-GIV were analyzed for β-COP, Gαi3 (a positive control), and EEA1 (a negative control) by immunoblotting (IB). **(E)** GST pull-down assays were carried out with lysates of COS7 cells transfected with pCEFL-GST-GIV or empty vector (pCEFL-GST) as above, and bound proteins were analyzed for β-COP and SEC13 by immunoblotting (IB). **(F)** Adeno-GIV-WT-HA or -GIV-FA-HA infected HeLa cells were prepermeabilized with 0.1% Saponin (to release cytosolic β-COP), stained for β-COP (red) and the nucleus (DAPI, blue), and analyzed by confocal microscopy as in **2H**. Bar = 10 μm. Quantification of the number of COPI vesicles per cell in **E**, as determined by 3D-reconstruction using Imaris software is shown in **Fig 2J**. **(G, H)** Neither depletion of GIV, nor expression of the GEF-deficient GIV-FA mutant alters the total level of cellular β-COP. **(G)** Whole cell lysates of control (Ctrl siRNA) or GIV-depleted (GIV siRNA) cells were analyzed for GIV, β-COP and tubulin by immunoblotting (IB). **(H)** Whole cell lysates of HeLa cells expressing HA-tagged GIV-WT or GIV-FA (adenoviral expression) were analyzed for HA, GIV, β-COP and tubulin by immunolotting (IB).

Supplementary Figure 3 (S3; related to Figure 2): Characterization of the β-COP-coated structures in the periphery of GIV-depleted cells. (A) Control (Ctrl siRNA) or GIV-depleted (GIV siRNA) COS7 cells were fixed, immunostained for β-COP (red) and GM130 (a marker of Golgi; green) and analyzed by confocal microscopy. The area of the cell periphery that was analyzed for the presence of β-COP-stained vesicular structures is indicated with an interrupted line. Images show that in control cells there is virtually no β-COP-stained puncta in the cell periphery and the GM130-stained Golgi membranes are compact. By contrast, in the GIV-depleted cells, there are multiple β-COP-stained puncta in the cell periphery, and that these puncta are distinct from the loosely arranged GM130-stained Golgi stacks. **(B)** Control (Ctrl siRNA) and GIV-depleted COS7 Cells (GIV siRNA) were fixed and immunostained for β-COP (red) ERGIC-53 (green) and analyzed by confocal microscopy. The images displayed here were constructed by merging of 10 optical slices (Z-scan), each 0.30 μm in thickness. A high magnification of the selected region (box) is shown in the right upper panel. The white line in the boxed region indicates the pixels used for the RGB profile plots shown in the right lower panel. In control cells ERGIC-53 is found in vesicular-tubular cluster scattered throughout the cytoplasm which do not stain for β-COP and only infrequently have β-COP-stained puncta at close proximity. By contrast, in GIV-depleted cells β-COP is found in punctate vesicular

structures (most likely COPI vesicles) scattered throughout the cytoplasm, frequently at close proximity to ERGIC-53-stained vesicular-tubular structures. RGB profiles on the right display the quantification of the frequency and intensity of red pixels (β-COP stained puncta) and their proximity to green pixels (ERGIC).

Supplementary Figure 4 (S4; related to Figure 4): GIV is required for the functional and structural integrity of the Golgi. (A) GIV and its GEF function is required for anterograde vesicle transport. GIV-depleted COS7 cells were infected with adenovirus containing siRNA-resistant GIV-WT-HA or GIV-FA-HA followed by transfection with VSV-G-ts045-GFP. Cells were incubated at 40°C overnight before shifting to 32°C for the indicated times. Cell surface proteins were labeled with membrane-impermeable Sulfo-NHS-SS-Biotin as described in *Experimental Procedures*. Surface biotinylated and total VSV-G-GFP were analyzed by immunoblotting with anti-GFP. Quantification (see **Figure 3C**) of VSV-G trafficking by band densitometry shows that expression of a GEF-deficient GIV-FA mutant slows down VSV-G trafficking from the ER to the PM. **(B)** HeLa cells stably expressing GIV-WT or GEF-deficient GIV-FA mutant were transfected with myc-Cochlin and then pulsed with [^{35}S]Met-Cys (100 mCi/mL) for 30 min, washed, and chased for the indicated times prior to lysis. Equal aliquots of media and cell lysates were incubated with anti-myc mAb and protein G agarose beads. Bound proteins were analyzed for [^{35}S]-labeled-Cochlin by autoradiography as in **Fig. 4D**. Quantification (see **Fig. 4F**) showed that secretion of myc-cochlin is delayed in cells expressing GIV-FA. **(C)** Control or GIV-depleted cells were transfected with VSV-G-ts045-GFP and incubated at 40°C overnight, shifted to 32°C for the indicated times, and then fixed and stained for GFP (white pixels). Representative images (Left) of cells at each time point are shown. Bar = 10 μm. Bar graphs (Right) display % of total VSV-G-GFP in the Golgi region (see details in Methods). Error bars represent mean ± S.E.M of 3 independent experiments (4 cells/experiment). Bar =10 μm. **(D)** Cells were transfected with Gαi3 WT or WF mutant and VSV-G-ts045-GFP as indicated, incubated at 40°C overnight, shifted to 32°C for the indicated times, and then fixed and stained for GFP (white pixels) and Gαi3 (not shown). Representative images of cells that were co-transfected with Gαi3 and VSV-G-ts045-GFP at each time point are shown. In control cells, strong staining is noted at the PM at 60 min, whereas in GIV-depleted cells, most of the VSV-G is still in transit within perinuclear compartments that represent dispersed Golgi cisternae. Bar = 10 μm. **(E)** COS7 cells infected with HA-tagged adeno-GIV-WT or -GIV-FA were transduced with VSV-G-tsO45 retrovirus for 1 hr at 32°C and shifted to 40°C for a further 16 hr. Cells were then shifted to 32°C

for 30, 60 and 120 min to allow movement of VSV-G protein from the ER towards the Golgi. Cells were lysed and incubated in the absence (-) or presence (+) of Endo-H. The Endo-H sensitive (lower band) and resistant (upper shift) forms of VSV-G were separated by SDS-PAGE and detected by immunoblotting using anti-VSV-G (upper panel). Anti-HA was used to confirm equal expression of GIV-WT or GIV-FA (lower panel). **(F-I)** Depletion of GIV (**F, I**) or expression of mutant GIV **(G)** or Gαi **(H)** proteins that cannot assemble GIV-Gαi complexes triggers dispersal of the Golgi cisternae. **(F)** Control (Ctrl siRNA) or GIV-depleted (GIV siRNA) HeLa cells were grown in 10% serum, fixed and stained for GM130, a *cis*-Golgi marker, (green, upper panel) or galactosyltransferase (green, GalT), a trans Golgi marker (lower panel) and nuclei (DAPI; blue), and analyzed by confocal microscopy. Representative images of control or GIV-depleted cells show that Golgi staining is distributed over a broader area in GIV-depleted cells than in controls, indicating partial dispersal of Golgi elements. Bar =10 μm. **(G, H)** HeLa cells expressing GIV (WT or FA mutant, **G**) or Gαi3 (WT or WF mutant, **H**) were fixed and stained for GM130 (green), Giantin (red), Gαi3-YFP (green) and nuclei (DAPI, blue) as indicated, and analyzed by confocal microscopy. Representative images of cells show that the Golgi is dispersed in cells expressing mutants of GIV or Gαi3 that cannot assemble a functional GIV-Gαi complex. Inset in panels **H** show the Giantin-stained Golgi stacks (red). Bar =10 μm. **(I)** Control (Ctrl siRNA) or GIV-depleted (GIV siRNA) HeLa cells were grown in 10% serum, fixed and analyzed by electron microscopy. In control cells (left) the Golgi (G) apparatus appears as a highly organized and compact structure in which stacks of flattened cisternae are tightly attached to each other in the juxtanuclear region. In GIV-depleted cells (right) the Golgi stacks (G) are more dispersed and the cisternae are organized into mini-stacks. Bar = 100 nm.

Supplementary Figure 5 (S5; related to Figure 5): GIV terminates Arf1 by targeting ArfGAP3 to COPI vesicles and releasing free Gβγ dimers. (A-C) GIV binds ArfGAP2/3 and is required for the localization of ArfGAP3 to the Golgi. **(A)** Equal aliquots of lysates of HEK293 cells coexpressing pCEFL-GST-GIV (right; 3 lanes) or GST alone (pCEFL-GST; left 3 lanes) and either ArfGAP2-HA or ArfGAP3-myc were incubated with glutathione-Sepharose beads and bound proteins (Upper, Bound) were analyzed for GST proteins and ArfGAPs 2 and 3 using HA (green) and myc mAbs (red), respectively, by dual color immunoblotting (IB). **(B)** ArfGAP3 colocalizes with β-COP. COS7 cells transfected with ArfGAP3-myc were fixed and stained for ArfGAP3 (anti-myc; green), endogenous β-COP (red) and the nucleus (DAPI; blue). β-COP and ArfGAP3 colocalize (yellow pixels) predominantly on the Golgi. Inset within the merged panel shows colocalization (arrowheads) also on vesicles away from the Golgi. Bar = 10 μM. **(C)**

Depletion of GIV reduces Golgi localization of ArfGAP3-myc, but not Arf1GAP1-myc. Control (Ctrl siRNA) or GIV-depleted (GIV siRNA) COS7 cells transfected with myc-tagged ArfGAP1 or ArfGAP3 were fixed and stained with anti-myc (green) or Man II (red) and analyzed by confocal microscopy. Yellow pixels in the merged panels on the right show that ArfGAP1 or ArfGAP3 staining overlaps with Man II in control cells. In GIV-depleted cells, only ArfGAP1 (left), but not ArfGAP3 (right) colocalized with Man II at the Golgi. Bar = 10 μM. **(D, E)** Sequestration of Gβγ heterodimers by βARK-CT delays ER to Golgi transport of VSV-G and triggers the dispersal of Golgi stacks. **(D)** COS7 cells expressing vector control or βARK-CT were infected with VSV-G-tsO45 retrovirus for 1 h at 32°C and shifted to 40°C for the next 16 h. Cells were then shifted to 32°C for 5, 30 and 60 min to allow movement of VSV-G protein from the ER to the Golgi prior to fixation. Fixed cells were stained for VSV-G-GFP (green), βARK-CT (red) and the nuclei (DAPI; blue). In vector-transfected control cells (upper panels) VSVG localizes predominantly to the ER at 40˚C (0 min), and upon temperature shift to 32˚C VSVG quickly moves from the ER to ERGIC (5 min), to the perinuclear Golgi compartment (30 min) and finally to the PM (60 min). In βARK-CT-transfected cells (lower panels) expressing cells, VSVG is predominantly localized to the ER at 5 min and trafficking towards Golgi is slowed down, and at 30 and 60 min most of the VSV-G is seen in the Golgi and does not reach the PM. Bar = 10 μM. **(E)** COS7 cells transfected with either vector control or βARK-CT were fixed and stained for βARK-CT (red), GM130 (Golgi marker; green) and nuclei (DAPI; blue) and visualized by confocal microscopy. Representative image panels are shown. The Golgi in vector-transfected control cells is compact, whereas in βARK-CT transfected cells it is dispersed. Bar = 10 μM.

Supplementary Figure 6 (S6; related to Figure 6): Active Arf1 binds GIV and triggers its membrane association. (A) Cos7 cells transfected with HA-tagged wild-type (WT) or constitutively active (Q71L) mutant Arf1 were fixed and stained for Arf1 (HA; green) and GIV (red) and nuclei (DAPI; blue). Golgi-localization of GIV is enhanced in cells expressing active Arf1 mutant, as determined by the intensity of staining. Bar = 10 μM. **(B)** Sequence alignment of GIV homologues reveal that the putative GGA-GAT like region within the Hook domain of GIV is evolutionarily conserved. The sequence corresponding to the N-terminal Hook domain of human GIV (BAE44387, aa 90–150) was used to identify homologues by BLAST search. The identified homologues with higher identity scores were aligned using CLUSTAL W. Conserved residues are shaded in black; similar residues in gray. This alignment reveals that the key amino acids that are essential for Arf1:GIV interaction are conserved in fish, birds and mammals alike

(highlighted in red or green). The residues marked with red star were mutated in this work to confirm that they are essential for the Arf1:GIV interaction.

Supplementary Figure 7 (S7; related to Figure 7): (A) ArfGAP3 is recruited to COPI vesicles independent of GIV's GEF function. COS7 cells infected with adeno-GIV-WT or -GIV-FA were subsequently transfected with ArfGAP3-Myc. Fixed cells were analyzed for interaction between ArfGAP3-Myc and β-COP (the major adaptor of COPI coatomer) by *in-situ* PLA using anti-myc and anti-β-COP antibodies. Red dots in image panels (left) indicate protein-protein interaction; Bar =10 μm. Bar graphs (right) display the quantification of interactions. Error bars represent mean ± S.E.M. of 3 independent experiments (>20 cells/experiment). Interaction between ArfGAP3 and β-COP, as determined by PLA signals/cell is equal in cells expressing GIV-WT and GIV-FA, indicating that the recruitment of ArfGAP3 on COPI vesicles is independent of GIV's GEF function. **(B)** ArfGAP3 is required for the termination of Arf1 activity by GIV-GEF function. HeLa cells stably expressing scramble or ArfGAP3 shRNA were depleted of endogenous GIV by siRNA, and were infected with adenoviral vectors expressing siRNA-resistant GIV-WT or GIV-FA as indicated. Equal aliquots of lysates of these cells (lower panels; input) were analyzed for Arf1:GTP by carrying out GST pulldown assays with GST-GGA3. Bound proteins (top panel) were analyzed for active Arf1 by immunoblotting (IB; Left). The efficacy of depletion of ArfGAP3 was confirmed as ~95% by immunoblotting. Similar levels of adenoviral expression of GIV-WT-HA or GIV-FA-HA was confirmed by dual color immunoblotting [an overlay of anti-GIV (red) and anti-HA (green) is shown]. Bar graphs (right) display the quantification of % bound Arf1:GTP/total Arf1 (Y Axis) in the various conditions tested. Arf1:GTP levels were increased in cells without a functional GIV-GEF (compare GIV-WT vs GIV-FA in Scr shRNA cells) as seen before in **Fig 3B**. No such increase was seen in cells depleted of ArfGAP3 (compare GIV-WT vs GIV-FA in ArfGAP3 shRNA cells). As expected, Arf1:GTP levels were increased in cells depleted of ArfGAP3 compared to Scr shRNA (compare GIV-WT in Scr shRNA cells vs GIV-WT in ArfGAP3 shRNA cells). Error bars represent mean ± S.E.M of 4 independent experiments. n.s. = not significant.

2. SUPPLEMENTARY FIGURES

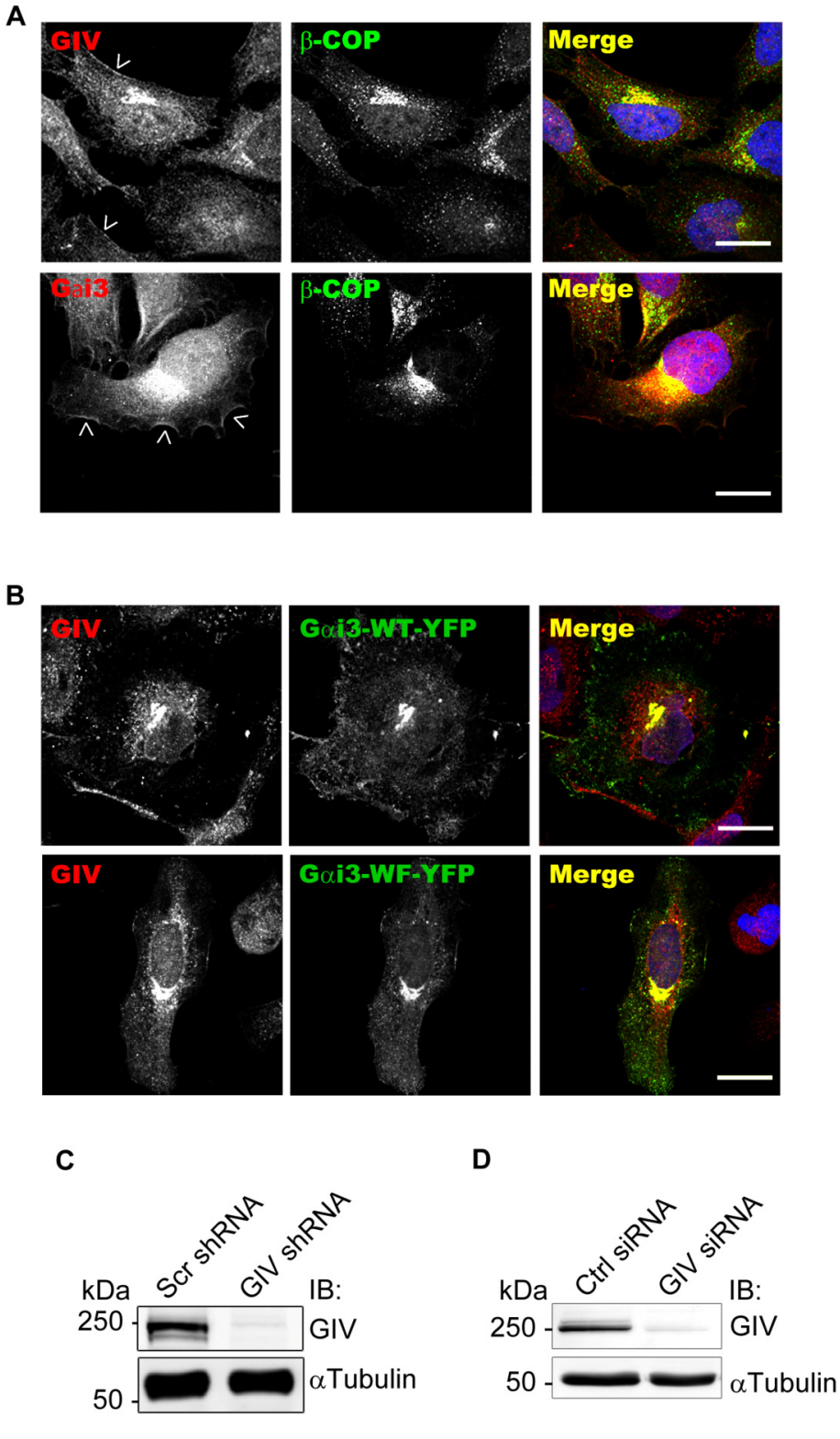

Figure S1: Related to Figure 1

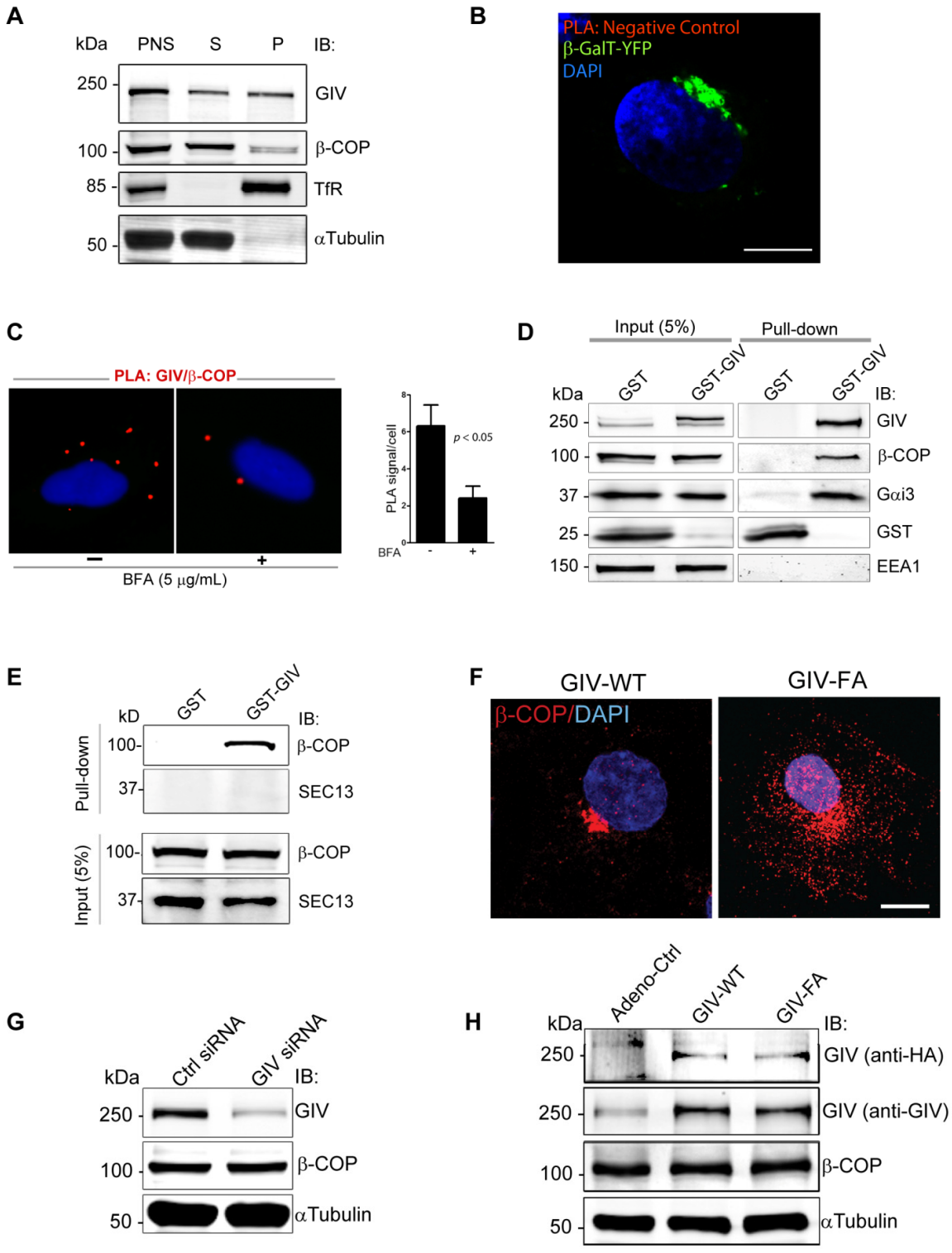

Figure S2: Related to Figure 2

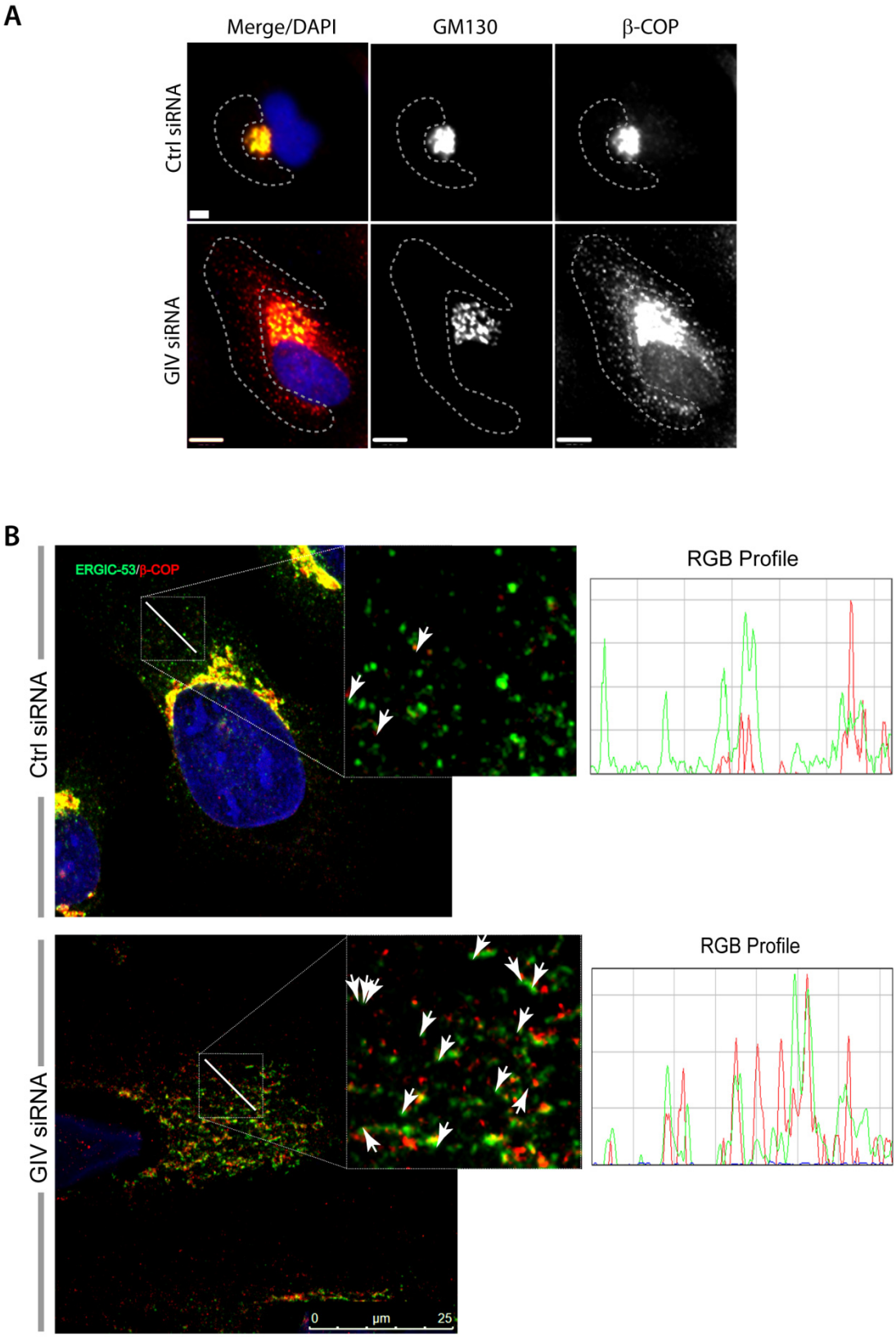

Figure S3: Related to Figure 2

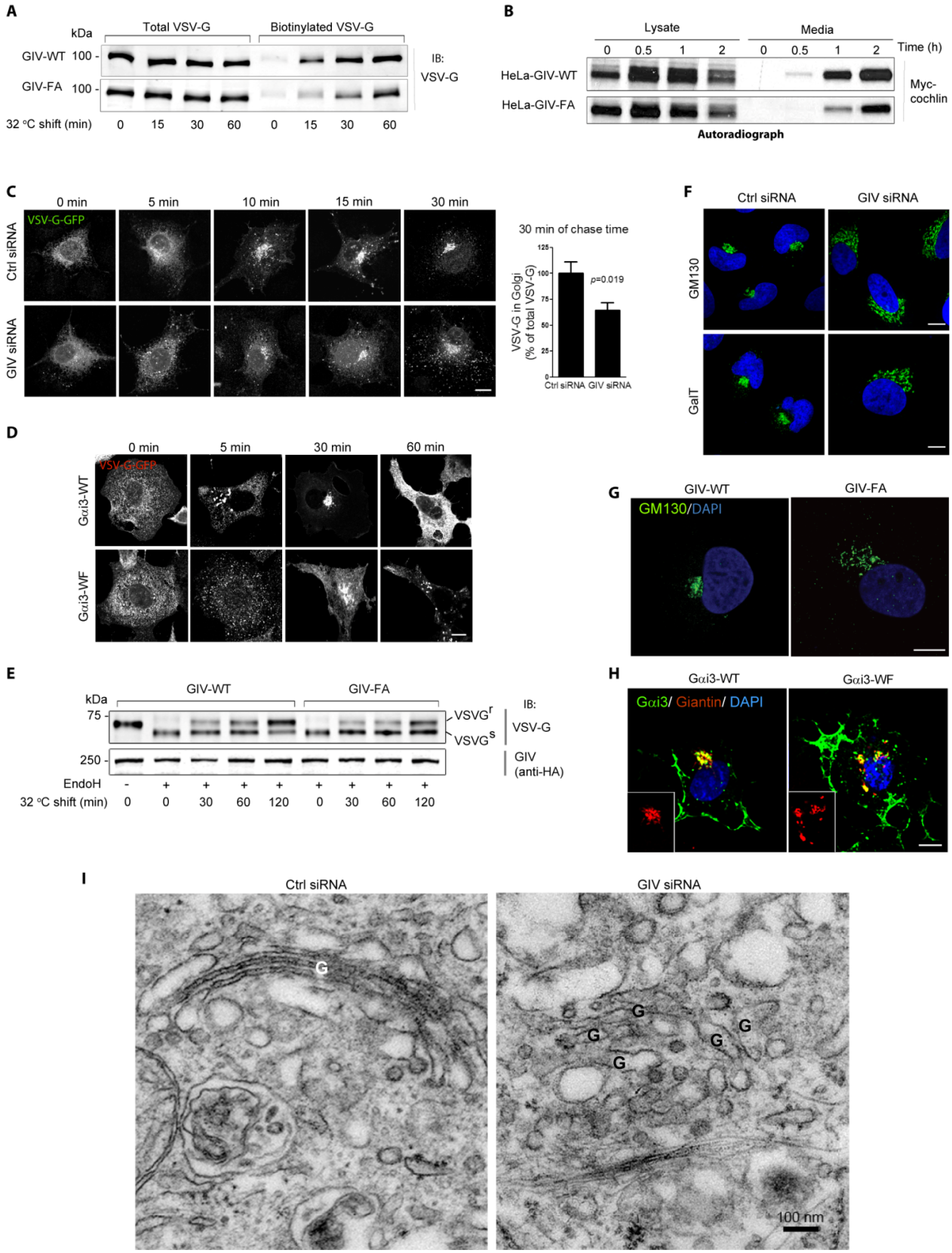

Figure S4: Related to Figure 4

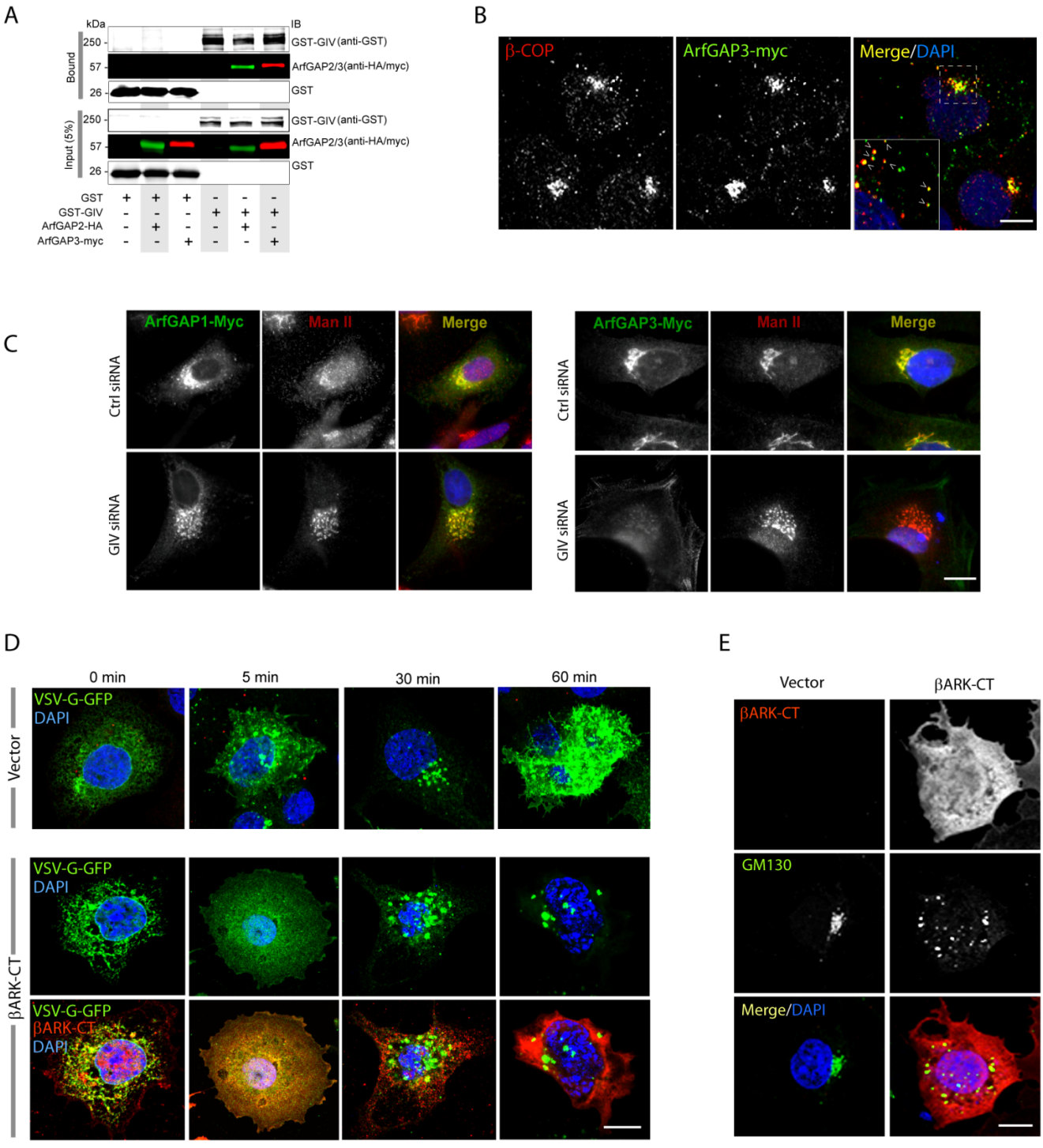

Figure S5: Related to Figure 5

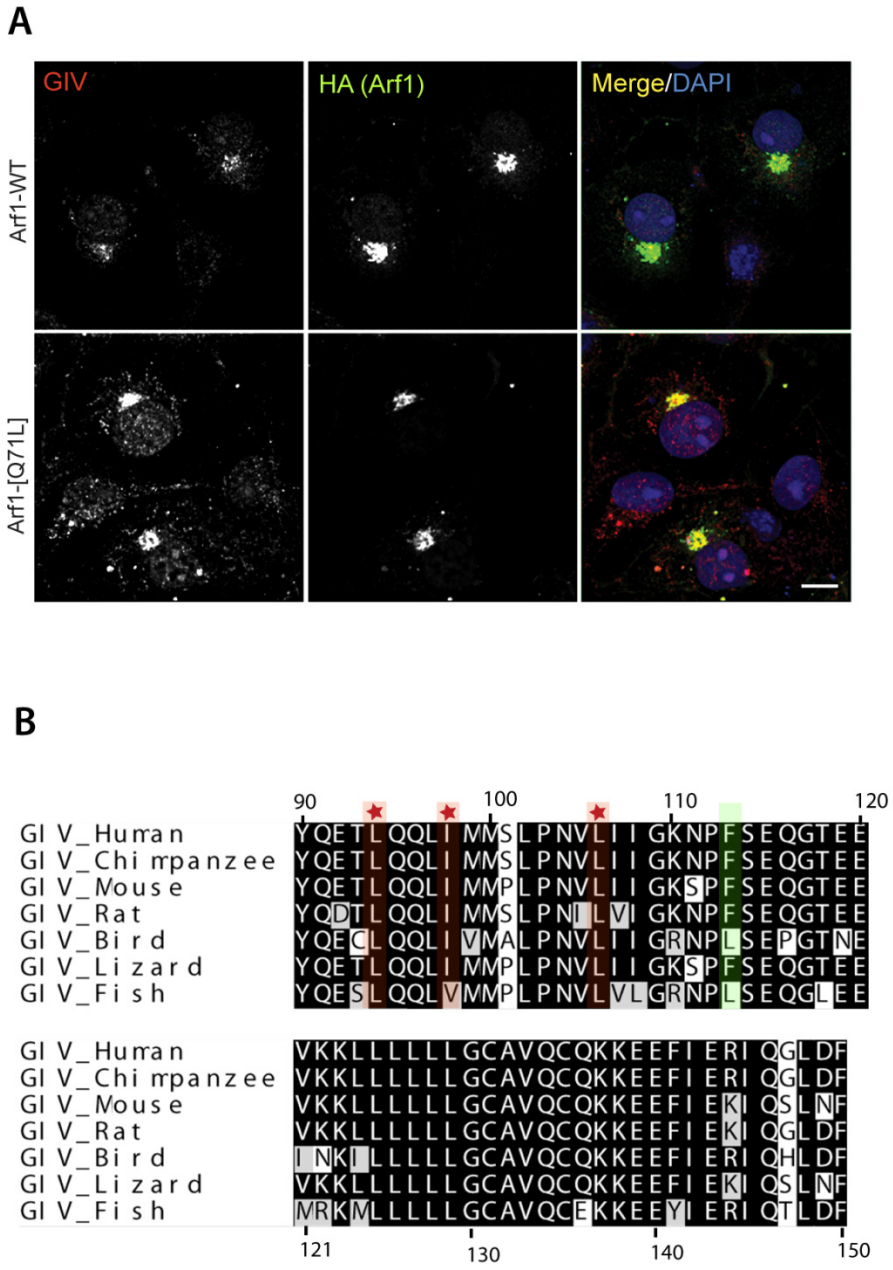

Figure S6: Related to Figure 6

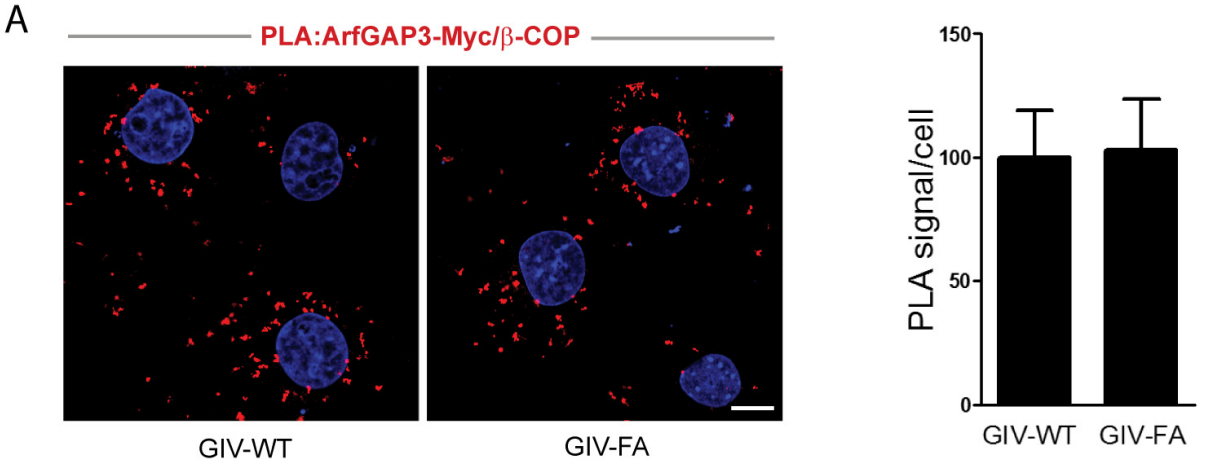

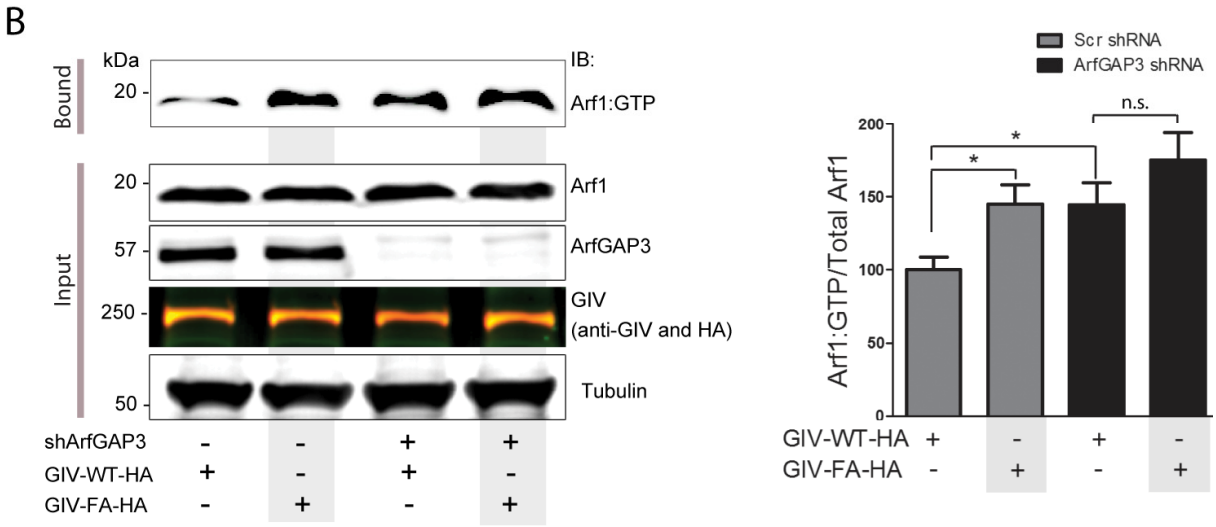

Figure S7: Related to Figure 7

3. SUPPLEMENTARY TABLES: None

4. SUPPLEMENTARY EXPERIMENTAL PROCEDURES

Reagents and antibodies: GIV siRNAs were obtained from Dharmacon (Lafayette, CO), Gαi3 siRNA from Santa Cruz Biotechnology (Santa Cruz, CA) and silencer Negative Control #1 siRNA from Ambion (Austin, TX). Rabbit anti-Girdin/GIV (GIV-CT) and Gαi3 IgGs were purchased from Santa Cruz Biotechnology, anti-GRK2 (βARK-CT) was from Sigma, anti-Giantin was from Covance Inc. A mouse mAb against the active conformation of Gαi was obtained from Dr. Graeme Milligan (University of Glasgow, UK). Rabbit anti-Arf1 IgG was prepared as described (Marshansky et al., 1997). Rabbit polyclonal anti-α-mannosidase II (Man II) serum was prepared as described (Velasco et al., 1993). Mouse and rabbit anti-β-COP antibodies were from Novus Biologicals (Littleton, CO) and Pierce (Rockford, IL), respectively. Other mouse mAbs were purchased as follows: GFP (Clontech, Mountain View, CA), HA and Giantin (Covance Research Products, Denver, PA), myc (Cell Signaling, Beverly, MA), Flag (Sigma, St. Louis, MO), LAMP-2 (Developmental Studies Hybridoma Bank, University of Iowa), GM130 (B.D. Biosciences), and α-tubulin (Sigma-Aldrich, St. Louis, MO). To detect Arf1, we used a rabbit polyclonal antibody obtained from R.A. Kahn (NIH) and extensively characterized previously (Zhang C-j, J Cell Biol, 1994). It was generated against a COOH-terminal peptide derived from human Arf1 and can specifically recognize Arf1, and not Arfs 3, 5 or 6. Control mouse IgGs used for immunoprecipitation were purchased from Cell Signaling Technology. Highly cross-absorbed Alexa Fluor 594 or 488 F(ab)′$_2$ fragments of goat anti-mouse or anti-rabbit IgG (H+L) for immunofluorescence were purchased from Invitrogen (Carlsbad, CA). Goat anti-rabbit and anti-mouse Alexa Fluor 680 or IRDye 800 F(ab)′$_2$ for immunoblotting, were obtained from LI-COR Biosciences.

Plasmids and viral constructs: RNAi-resistant GIV provided by M. Takahashi (Nagoya University School of Mediine) was subcloned into a pcDNA 3.1 and pCEFL-GST vectors. Cloning of wild-type rat Gαi3 cDNA, Gαi3-Q204L, and Gαi3-G203A mutants into pcDNA 3.1 were described previously (Ghosh et al., 2008). GIV-F1685A and Gαi3-W258F mutants were generated as described previously (Garcia-Marcos et al., 2009; Lane et al., 2008). Arf1-HA, ARF1-Q71L-HA were prepared as previously described (Uslu and Bonavida, 1995). βARK-CT was provided by R. J. Lefkowitz (Duke University, Durham, NC). Wild-type GIV and the GIV-

F1685A mutant were subcloned into the pAdEasy adenoviral expression system (Stratagene, Santa Clara, CA). GST-GGA3 was from Julie Donaldson (National Institutes of Health, Bethesda, MD).

Cell culture, transfection and infection: HeLa and COS7 (American Type Culture Collection, Manassas, VA) were maintained in DMEM (Invitrogen) supplemented with 10% FBS (Hyclone, Logan, UT), 100 U/ml penicillin, 100 µg/ml streptomycin, 1% L-glutamine and 5% CO2. For transfection of siRNA oligos, HeLa or COS7 cells were seeded (1×10^5 cells/35 mm dish or 7×10^5 cells/10 cm dish), and 24 h later they were transfected with 20 nM siRNA for 14 h using Oligofectamine (Invitrogen) according to the manufacturer's instructions. When reversal of phenotype was attempted, cells were infected with HA-tagged adeno-GIV wild-type or F1685A mutant (>10 pfu/cell) 12-16 h after-siRNA transfection and analyzed after ~38-40 h. Transfection of cells with plasmids was carried out using transit-LT1 (Mirus Bio, Madison, WI) following the manufacturer's protocol.

GST pull-down assays and immunoprecipitation: For most of the pull-down experiments, cells were grown in 100-mm dishes and transfected with different fusion proteins in mammalian expression vectors. Whole-cell extracts were prepared 48 h after transfection by resuspending the cells in lysis buffer (0.4% Triton X-100, 20 mM HEPES (pH 7.2), 5 mM Mg-acetate, 125 mM K-acetate, 1 mM DTT) supplemented with 100 mM sodium orthovanadate, with Complete Protease Inhibitor cocktail (Roche) and Phosphatase Inhibitor Cocktail 2 (Sigma-Aldrich). To bring down the fusion protein with its associated proteins, lysates were mixed with glutathione-Sepharose beads (G.E. Healthcare) for 12 h at 4°C with gentle shaking. The beads were extensively washed with lysis buffer followed by SDS-PAGE and immunoblotting.

For Arf1/GIV *in vitro* binding assay, sepharose-bound GST or GST-GIV proteins were obtained from HEK293T cells transiently transfected with pCEFL-GST or pCEFL-GST-GIV as described above. Lipid micelles were made freshly using a lipid compound Dimethyl pyrocarbonate, pyrocarbonic acid dimethyl ester (DMPC) as 30 mM solution in 20 mM HEPES, 1 mM EDTA and 2 mM $MgCl_2$ by ultra-sonication until it became clear. Purified myristoylated Arf1 (2.5µg) was loaded with GDP (50 µM) or GMP-PNP (50 µM) in the presence of lipid micelles (final 3 mM) in binding buffer (25 mM HEPES, pH 7.4, 100 mM NaCl, 1 mM EDTA, 0.5 mM $MgCl_2$, 1 mM DTT, 0.1% sodium cholate) at 30 ^oC for 1 h followed by incubation with sepharose-bound GST-GIV or GST at 40 ^oC for 4 h. Beads were washed and boiled in Laemmli

sample buffer, and bound proteins were analyzed by immunoblotting with anti-GST and anti-Arf1 IgG.

For immunoprecipitation, cells were harvested, suspended in lysis buffer, homogenized, incubated on ice for 10 min, and cleared by centrifugation (13,000 *g* for 10 min). Cell extracts were incubated overnight at 4°C with anti-FLAG, anti-Myc or control IgG. Protein G–Sepharose beads (GE Health Sciences) were added and incubated for an additional 2 h. Beads were washed and boiled in Laemmli sample buffer for 5 min, and bound proteins were analyzed by immunoblotting.

Arf activation assays: Purification of GST-GAT protein and assessment of Arf1 activation were described previously (Cohen and Donaldson, 2010). In brief, cells were lysed with 1% Triton X-100, 50 mM Tris, pH 7.5, 100 mM NaCl, 2 mM $MgCl_2$, 0.1% SDS, 0.5% sodium deoxycholate, 10% glycerol with protease inhibitors. Equal amounts of lysates were incubated with GST-GGA3 (~40 μg) prebound to glutathione-Sepharose 4B beads at 4°C for 1 h. Beads were washed, and the bound proteins were eluted by boiling in Laemmli sample buffer for 5 min, resolved on a 15% SDS-PAGE, and analyzed by immunoblotting.

Immunofluorescence, proximity Ligation (PLA), and FRET assays: For immunofluorescence, cells grown on coverslips were fixed in 3% paraformaldehyde (PFA) and processed as described previously (Ghosh et al., 2010). Antibody dilutions were as follows: GIV, β-COP, GM130, 1:100; myc, GFP, 1:500; ERGIC-53, Man II, 1:800; goat anti-mouse or anti-rabbit Alexa 488 or Alexa 594, 1:500. DAPI was used at 1:10,000. To estimate the degree of colocalization in immunofluorescence assays, ImageJ RGB Profiler plugin was used to determine the intensity fluorescence distribution for corresponding fluorophore (green and red channels).

For PLA, cells were processed according to the manufacturer's instructions. Antibody dilutions were the same as for immunofluorescence. Images were acquired using a Leica Confocal microscope with a 63X oil objective. For analyzing the number of objects, a fixed threshold was applied to all images using NIH Image, and the number of objects and total fluorescence measured using the Analyze Particles function.

For FRET studies, previously validated internally tagged $G\alpha i_1$-YFP and CFP-$G\beta_1$ FRET probe pairs were used (Bunemann et al., 2003; Gibson and Gilman, 2006). Control (Sh-Scr) or GIV depleted (sh-GIV) COS7 stable cells cultured in glass bottom dishes were transfected with 2 μg each of $G\alpha i_1$-YFP, CFP-$G\beta_1$, and $G\gamma_2$ constructs. After 48 h of transfection, cells were

imaged in DMEM media without phenol red using an Olympus IX91 inverted confocal microscope (UCSD Light Microscopy Core). FRET efficiency was calculated on a pixel by pixel basis from the normalized ratiometric images obtained individually in donor, FRET and acceptor channels. For FRET quantification, regions of interest (ROI) were drawn in the juxtanuclear area presumably in the Golgi region to compute energy transfer. Individual cells with fluorescence intensity in the mesoscopic regime detected in the donor and acceptor channels were selected for FRET analysis to avoid inhomogeneities between samples (Midde et al., 2013; Midde et al., 2014)

GFP-tsO45-VSVG transport assays: To monitor anterograde (ER to Golgi) trafficking COS7 cells were treated overnight with control or GIV siRNA and transiently transfected with GFP-tsO45-VSV-G plasmid (Presley et al., 1997). Transfected cells were incubated for 14–16 h at the restrictive temperature (40°C) to accumulate VSV-G protein in the ER, shifted to 32°C for 0-60 min to release VSV-G protein and then fixed and processed for immunofluorescence. The rate of VSV-G trafficking from the ER to the Golgi was determined by calculating the ratio of Golgi-associated VSV-G, determined by colocalization with Man II, and total VSV-G fluorescence, using NIH Image software. Alternatively, acquisition of Endo H resistance was monitored (Griffiths et al., 1985). Briefly, COS-7 cells stably expressing control or GIV shRNA or COS-7 cells stably expressing GIV-WT or GIV-FA were infected with tsO45-VSV-G retrovirus for 1 h at 32 C and incubated for 16 h at 40°C. Cycloheximide (100 μg/mL) was added during the last hour. Cells were then shifted to 32°C for 0-90 min, followed by resuspension in lysis buffer (50 mM Tris, pH 7.5, 150 mM NaCl, 1% Triton X-100 with protease inhibitors). Cell extracts (10-15 μg protein) were digested with 5 mU Endo-H (New England Biolabs, MA) for 16 h at 37°C according to the manufacturer's protocol and analyzed by immunoblotting using anti-VSV-G IgG.

To assess COPI-dependent retrograde trafficking (Golgi to ER), control or GIV siRNA treated COS7 cells were transiently transfected with cDNA for tsO45-VSV-G-KDELr-Myc (Cole et al., 1998) and incubated for 24 h at 32°C, followed by 1 h at 32°C in the presence of cycloheximide (50 μg/ml), after which the cells were shifted to 40°C, fixed at different time periods and processed for immunofluorescence.

Surface biotinylation assays: Surface biotinylation of VSV-G at the PM was described previously (Lisanti et al., 1988). Briefly, cells were washed with ice-cold PBS twice and incubated with cell-impermeable Sulfo-NHS-SS-Biotin (sulfosuccinimidyl-2-(biotinamido) ethyl-

1,3-dithiopropionate; Pierce) at 4°C for 30 min. Cells were then lysed, and biotinylated proteins were immobilized on NeutrAvidin beads (Pierce) at 4°C for 2 h. Bound proteins were eluted with Laemmli sample buffer supplemented with 100 mM dithiothreitol at 95°C for 5 min and immunoblotted with anti-GFP IgG to detect GFP-tsO45-VSVG .

Metabolic labeling of myc-cochlin secretion: Metabolic labeling with ^{35}S-labeled cysteine-methionine and assessment of myc-cochlin secretion was done exactly as described previously (Styers et al., 2008).

Cell fractionation and immunoisolation: Membrane (100,000 *g* pellet) and cytosolic (100,000 *g* supernatant) fractions were prepared from postnuclear supernatants of HeLa or COS7 cells as previously described (Beas et al., 2012). Equal sample volume from cytosolic and membrane fractions were resuspended in 6X Laemmli sample buffer and analyzed by immunoblotting.

For immunoisolation of COPI vesicles, the membrane fraction (100,000 *g* pellet) was resuspended in 25 mM Tris-HCl pH 7.4, 100 mM NaCl, 1 mM EDTA, homogenized by passage (30X) through a 25-gauge needle and centrifuged at 13,000 g for 10 min. The supernatants were incubated overnight at 4°C with CM1A10 antibody against the native coatomer (a gift from James Rothman, Yale University) (Palmer et al., 1993) or control IgG. Protein G–Sepharose beads were added for 2 h, and bound proteins analyzed by immunoblotting.

For differential centrifugation, cells were resuspended in homogenization buffer (0.25 M sucrose, 1 mM EDTA, 10 mM KCl, 1.5 mM $MgCl_2$, 10 mM Hepes-NaOH, pH 7.4, with protease and phosphatase inhibitors) and disrupted by 6 passages through a ball-bearing homogenizer. The homogenate was cleared by centrifugation at 1,000 *g* for 10 min at 4°C, and the resulting postnuclear supernatant was successively centrifuged at 15,000 *g* for 20 min to yield a P2 fraction, 100,000 *g* for 60 min to yield a crude vesicle fraction (P3), and a cytosolic fraction. Fractions were analyzed by immunoblotting and the level of β-COP in the vesicle fraction (P3) was measured and expressed as a percentage of that in the whole cell lysates.

Lentivirus Production and Infection of COS7 Cells: The scramble and GIV shRNA constructs were from M. Garcia-Marcos (Boston University, Boston, Ma). The lentiviral packaging plasmid psPAX2 and envelope plasmid pMD2G were obtained from Dr. Chris Glass, UCSD. To prepare virus stocks, 293T cells were co-transfected with shRNA constructs, together with psPAX2 and pMD2G constructs (4:3:1 ratio, respectively), using transit-LT1 (Mirus Bio, Madison, WI). The medium was changed after 24 h, and virus-containing medium was collected

after 36–48 h. The viral stocks were centrifuged and filtered through a 0.45-μm filter to remove any nonadherent 293T cells. Cultures of COS7 cells or transfected COS7 cells were infected with a mixture of 0.5 ml of shRNA lentivirus-containing medium and 0.5 ml DMEM with 10% FBS. The medium was changed 24 h post-infection and replaced with fresh DMEM.

Transmission electron microscopy: Samples were fixed, stained in block in uranyl acetate, and embedded in Embed 812 resin, cut, and sections viewed using a JEOL 1200EX II transmission electron microscope (UCSD Electron Microscopy Core), and photographed using a Gatan Orius 600 digital camera. Pixel size was calibrated by Pelco grating replica #607 (Ted Pella, Inc.), with measurements performed in ImageJ.

Construction of a 3D model of Arf1 interaction with the N-terminal helix-loop-helix motif of GIV. The homology model of the Arf1:GIV complex was constructed using ICM comparative (homology) modeling procedure (Cardozo et al., 1995) using the structure of constitutively active Arf1 in complex with the N-terminal GAT domain of human GGA1 (PDB 1j2j) as a template and guided by the GIV/GGA1 sequence alignment in **Fig 6G**. The initial model was by assigning the backbone coordinates of both target molecules (Arf1 and GIV) to their counterparts in the template; this model was further refined using extensive sampling of residue side chains in internal coordinates and then additionally relaxed by full-atom local minimization in the presence of distance restraints maintaining the conserved hydrogen bonds and thus protein secondary structure and topology.

Statistical Analysis: Each experiment presented in the figures is representative of at least three independent experiments. Statistical significance between the differences of means was calculated by unpaired student's t-test. A two tailed p value of <0.05 at 95% confidence interval is considered as statistically significant. All graphical data presented were prepared using GraphPad or Matlab softwares.

5. SUPPLEMENTARY REFERENCES

Beas, A.O., Taupin, V., Teodorof, C., Nguyen, L.T., Garcia-Marcos, M., and Farquhar, M.G. (2012). Galphas promotes EEA1 endosome maturation and shuts down proliferative signaling through interaction with GIV (Girdin). Mol Biol Cell *23*, 4623-4634.

Bunemann, M., Frank, M., and Lohse, M.J. (2003). Gi protein activation in intact cells involves subunit rearrangement rather than dissociation. Proc Natl Acad Sci U S A *100*, 16077-16082.

Cardozo, T., Totrov, M., and Abagyan, R. (1995). Homology modeling by the ICM method. Proteins *23*, 403-414.

Cohen, L.A., and Donaldson, J.G. (2010). Analysis of Arf GTP-binding protein function in cells. Curr Protoc Cell Biol *Chapter 3*, Unit 14 12 11-17.

Cole, N.B., Ellenberg, J., Song, J., DiEuliis, D., and Lippincott-Schwartz, J. (1998). Retrograde transport of Golgi-localized proteins to the ER. J Cell Biol *140*, 1-15.

Garcia-Marcos, M., Ghosh, P., and Farquhar, M.G. (2009). GIV is a nonreceptor GEF for G alpha i with a unique motif that regulates Akt signaling. Proceedings of the National Academy of Sciences of the United States of America *106*, 3178-3183.

Ghosh, P., Beas, A.O., Bornheimer, S.J., Garcia-Marcos, M., Forry, E.P., Johannson, C., Ear, J., Jung, B.H., Cabrera, B., Carethers, J.M*., et al.* (2010). A G{alpha}i-GIV molecular complex binds epidermal growth factor receptor and determines whether cells migrate or proliferate. Mol Biol Cell *21*, 2338-2354.

Ghosh, P., Garcia-Marcos, M., Bornheimer, S.J., and Farquhar, M.G. (2008). Activation of Galphai3 triggers cell migration via regulation of GIV. J Cell Biol *182*, 381-393.

Gibson, S.K., and Gilman, A.G. (2006). Gialpha and Gbeta subunits both define selectivity of G protein activation by alpha2-adrenergic receptors. Proc Natl Acad Sci U S A *103*, 212-217.

Griffiths, G., Pfeiffer, S., Simons, K., and Matlin, K. (1985). Exit of newly synthesized membrane proteins from the trans cisterna of the Golgi complex to the plasma membrane. J Cell Biol *101*, 949-964.

Lane, J.R., Henderson, D., Powney, B., Wise, A., Rees, S., Daniels, D., Plumpton, C., Kinghorn, I., and Milligan, G. (2008). Antibodies that identify only the active conformation of G(i) family G protein alpha subunits. FASEB J *22*, 1924-1932.

Lisanti, M.P., Sargiacomo, M., Graeve, L., Saltiel, A.R., and Rodriguez-Boulan, E. (1988). Polarized apical distribution of glycosyl-phosphatidylinositol-anchored proteins in a renal epithelial cell line. Proceedings of the National Academy of Sciences of the United States of America *85*, 9557-9561.

Marshansky, V., Bourgoin, S., Londono, I., Bendayan, M., and Vinay, P. (1997). Identification of ADP-ribosylation factor-6 in brush-border membrane and early endosomes of human kidney proximal tubules. Electrophoresis *18*, 538-547.

Midde, K., Rich, R., Marandos, P., Fudala, R., Li, A., Gryczynski, I., and Borejdo, J. (2013). Comparison of orientation and rotational motion of skeletal muscle cross-bridges containing phosphorylated and dephosphorylated myosin regulatory light chain. J Biol Chem *288*, 7012-7023.

Midde, K., Rich, R., Saxena, A., Gryczynski, I., Borejdo, J., and Das, H.K. (2014). Membrane topology of human presenilin-1 in SK-N-SH cells determined by fluorescence correlation spectroscopy and fluorescent energy transfer. Cell biochemistry and biophysics *70*, 923-932.

Palmer, D.J., Helms, J.B., Beckers, C.J., Orci, L., and Rothman, J.E. (1993). Binding of coatomer to Golgi membranes requires ADP-ribosylation factor. J Biol Chem *268*, 12083-12089.

Presley, J.F., Cole, N.B., Schroer, T.A., Hirschberg, K., Zaal, K.J., and Lippincott-Schwartz, J. (1997). ER-to-Golgi transport visualized in living cells. Nature *389*, 81-85.

Styers, M.L., O'Connor, A.K., Grabski, R., Cormet-Boyaka, E., and Sztul, E. (2008). Depletion of beta-COP reveals a role for COP-I in compartmentalization of secretory compartments and in biosynthetic transport of caveolin-1. Am J Physiol Cell Physiol *294*, C1485-1498.

Uslu, R., and Bonavida, B. (1995). Free-radicals dependent and independent pathways of cddp-mediated cytotoxicity and apoptosis in ovarian tumor-cell lines. International journal of oncology *6*, 1003-1009.

Velasco, A., Hendricks, L., Moremen, K.W., Tulsiani, D.R., Touster, O., and Farquhar, M.G. (1993). Cell type-dependent variations in the subcellular distribution of alpha-mannosidase I and II. J Cell Biol *122*, 39-51.